

# Research and Development Towards an Autonomous Biped Walking Robot

Dirk Wollherr

Martin Buss

Control Systems Group  
 Technical University of Berlin  
 Einsteinufer 17, EN11, D-10587 Berlin, Germany  
 Tel: +49-30-314-22945 Fax: +49-30-314-21137  
 www.rs.tu-berlin.de  
 Dirk.Wollherr@tu-berlin.de M.Buss@ieee.org

Michael Hardt

Oskar von Stryk

Simulation and Systems Optimization Group  
 Technische Universität Darmstadt  
 Alexanderstr. 10, D-64283 Darmstadt, Germany  
 Tel: +49-6151-162513 Fax: +49-6151-166648  
 www.sim.informatik.tu-darmstadt.de  
 {hardt, stryk}@sim.tu-darmstadt.de

## Abstract

*Methods for modeling, simulation and optimization of the dynamics, stability, and performance of humanoid robots are presented in this paper. Optimal control trajectory following by joint-level control combined with an online compensation method using Jacobians is proposed. The kinematic design, dynamic properties, hard- and software architecture for an autonomous biped, and experimental results are presented.*

## INTRODUCTION

Three key issues are to be considered in the design of an autonomous biped robot: (i) the functional and physical requirements derived from the envisioned application area; (ii) the selection and integration of hardware (HW) and software (SW) suited to meet these requirements; (iii) the development and integration of efficient algorithms on all levels of control, planning, and perception subject to the real-time constraints given by the robot HW and SW design.

Many research groups and companies are developing biped walking machines, e.g. [1, 3, 5, 11–13]. However, towards the development of an effective autonomous robot, all of the three areas mentioned above must be considered. Especially for the development of *dynamic* biped locomotion, we find it important to model and simulate the biped locomotion dynamics on all levels of the design, implementation and operation phases of a humanoid robot, e.g. for the selection of motors and gears, or to obtain optimal step/stride trajectories. Contribution of this paper is a strategy for precise modeling of legged locomotion systems requires high dimensional non-linear multibody systems (MBS) dynamics with constraints. Issues addressed are the generation, optimization, and control of stable motions for humanoid robots. The paper proposes a novel online compensation method using Jacobians to influence the posture of the humanoid robot in selected cartesian task coordinate directions. Experimental results confirm the efficacy of our modeling, optimization, and online compensation approach to humanoid walking.

## MODELING OF DYNAMIC BIPED LOCOMOTION

### General considerations

Various approaches exist for modeling the MBS dynamics of a tree-structured legged robot subject to unilateral contact

constraints. Symbolic methods are required for closed-form dynamic equations which give the best performance in terms of number of arithmetic operations and basic function evaluations needed for evaluation. This approach, though, does not fulfill the need for modularity and flexibility if parts of the kinematical structure or the kinematical data have to be changed and refined as occurs frequently during the design and operation cycle of a humanoid robot. The MBS modeling and computational approach chosen is the Articulated Body Algorithm (ABA) due to its superior modularity and computational efficiency for high dimensional systems [4, 16].

The basic equations of motion for a humanoid robot are those for a rigid, multibody system experiencing contact forces

$$\begin{aligned}\ddot{\mathbf{q}} &= \mathcal{M}(\mathbf{q})^{-1} \left( B\mathbf{u} - \mathcal{C}(\mathbf{q}, \dot{\mathbf{q}}) - \mathcal{G}(\mathbf{q}) + J_c(\mathbf{q})^T \mathbf{f}_c \right) \\ 0 &= \mathbf{g}_c(\mathbf{q})\end{aligned}\quad (1)$$

where  $N$  is the number of links in the system,  $\mathcal{M} \in \mathbb{R}^{N \times N}$  is the square, positive-definite mass-inertia matrix,  $\mathcal{C} \in \mathbb{R}^N$  contains the Coriolis and centrifugal forces,  $\mathcal{G} \in \mathbb{R}^N$  the gravitational forces, and  $\mathbf{u}(t) \in \mathbb{R}^m$  are the control input functions which are mapped with the constant matrix  $B \in \mathbb{R}^{N \times m}$  to the actively controlled joints. The ground contact constraints on the system are  $\mathbf{g}_c \in \mathbb{R}^{n_c}$  from which the constraint Jacobian may be obtained  $J_c = \frac{\partial \mathbf{g}_c}{\partial \mathbf{q}} \in \mathbb{R}^{n_c \times N}$ , while  $\mathbf{f}_c \in \mathbb{R}^{n_c}$  is the ground constraint force.

A great advantage in legged systems is that their constrained contact legs often have unique inverse kinematic solutions, which can be used to derive reduced dynamic equations. This approach, also known as coordinate partitioning [2], projects the dynamics (1) onto a reduced set of independent states thus converting the DAE contact system (1) into an ODE system of minimal size. Using a recursive multibody algorithmic approach, the reduced dynamics may be evaluated without explicitly constructing them [8]. The constant mapping  $Z \in \mathbb{R}^{(N-n_c) \times N}$  from the full state vector  $\mathbf{q}$  to the independent states  $\mathbf{q}_I$  then reduces the dimension of the equations of motion and the system evolution follows automatically the contact manifold. The dependent states  $\mathbf{q}_D$  can be calculated from  $\mathbf{q}_I$ . A partition of the states as  $\mathbf{q} = (\mathbf{q}_I, \mathbf{q}_D)$  exists that

$$\ddot{\mathbf{q}}_I = Z\mathcal{M}(\mathbf{q})^{-1} \left( B\mathbf{u} - \mathcal{C}(\mathbf{q}, \dot{\mathbf{q}}) - \mathcal{G}(\mathbf{q}) + J_c^T \mathbf{f}_c \right) \quad (2)$$

holds. The principal advantage of this approach is that one needs only perform the optimization on the reduced dimensional state.

An important aspect of formulating a gait optimization problem is establishing the many constraints on the problem. For a biped, the gait cycle consists of several phases describing different contact situations and being separated by events. The order of contact events is straightforward and depends primarily upon the speed of locomotion. A summary of the modeling constraints for a *complete* gait cycle is [9]:

*Periodic gait constraints* (gait optimization):

- Periodicity of continuous state and control variables.
- Periodicity of ground contact forces.

*Exterior environmental constraints:*

- Kinematic constraints on the height ( $z$ -coordinate) of the swing leg tips.
- Ground contact forces lie within the friction cone and unilateral contact constraints are not violated.

*Interior modeling constraints:*

- Jump conditions in the system velocities due to inelastic collisions of the legs with the ground.
- Magnitude bounds on states, controls and control rates.
- Actuator torque-speed limitations.

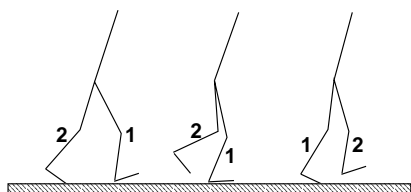


**Figure 1. Three Phases of Dynamic Gait with Different Foot Contact Positions for Leg 1: (1) Heel Roll, (2) Flat Contact, (3) Toe Roll**

Depending upon whether a statically stable or dynamically stable biped gait is desired, the optimization problem formulation will have different periodicity, symmetry, and kinematic phase boundary constraints depending on the foot contact positions (Fig. 1). The number of phases may also differ. We model the static and dynamically stable gaits as follows.

*Statically Stable Gait:*

- Phase 1: Foot 1 flat contact, Foot 2 swinging freely
- Phase 2: Foot 1 flat contact, Foot 2 flat contact

*Dynamically Stable Gait:*

- Phase 1: Foot 1 heel roll contact, Foot 2 toe roll contact
- Phase 2: Foot 1 flat contact, Foot 2 swinging freely
- Phase 2: Foot 1 toe roll contact, Foot 2 swinging freely

### Dynamic model of humanoid robot

As an example, we consider our humanoid currently under development, see Fig. 2 and Fig. 4.

The humanoid construction consists of:

- two legs each with 6 links and 6 actuated joints
- hip has 3 DoF, knee 1 DoF, ankle 2 DoF

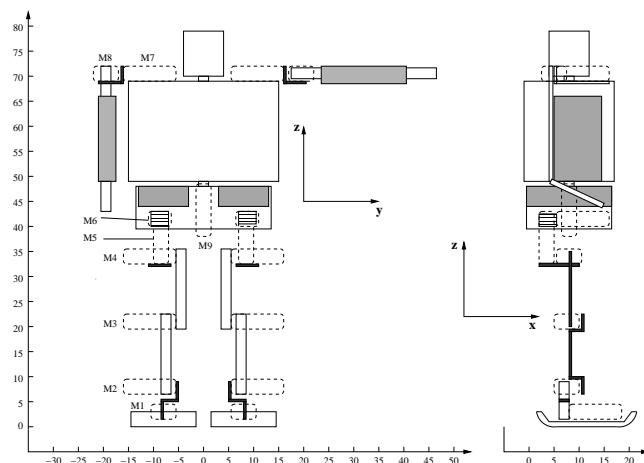


**Figure 2. Humanoid Kinematic Structure**

- waist joint providing a rotation about vertical axis
- each shoulder with 2 DoF
- head is (temporarily) fixed to the body

The humanoid dynamic model consists of:

- 17 degrees of freedom
- free-floating body with central reference point in the torso and a fictitious 6 DoF joint between it and an inertial reference frame
- modeled as a tree structured multibody system (contacts are "cut" between robot and ground)

If we restrict motion to the sagittal plane, a minimum set of generalized coordinates consists of 14 position and 14 velocity states ( $\mathbf{q}(t)$ ,  $\dot{\mathbf{q}}(t)$ ), thus a total of 28 first order differential equations. Then the free-floating fictional joint has only 3 DoF and each leg also only 3 DoF. With 3-dimensional motion, there are 23 position and 23 velocity states ( $\mathbf{q}(t)$ ,  $\dot{\mathbf{q}}(t)$ ) resulting in 46 differential equations.

### DYNAMIC STABILITY AND PERFORMANCE

#### Measures for dynamically stable locomotion

The notion of *static stability*, often used to enforce *postural stability* in legged systems, does not suffice for fast motion as targeted by this work. Static stability requires the ground projected center of gravity to lie within the *support polygon*, the convex hull about the leg contact points. This highly conservative measure of postural stability generally results in very slow legged motions. The notion of *dynamic stability* is required for faster legged motion, yet as pointed out in [6], a dynamically stable gait is one without static stability that is sustainable indefinitely.

The ZMP is that point on the ground where the total moment generated due to gravity and inertia equals zero or equivalently the point where the net vertical ground reaction force acts. This point has frequently been used to produce stable locomotion beyond the region of static stability [14]. This measure has many deficiencies when considering fast locomotion; in particular, it provides little stability information during the important rolling action of the feet (see Fig. 1)

in fast walking and running. The support polygon may then have a zero or reduced surface area, and the ZMP may lie directly on the support boundary, thus on the border of its pre-defined stability region.

A stability measure related to the ZMP providing more information as to the system instability was presented in [6]. This FRI point or foot-rotation indicator coincides with the ZMP during periods of static equilibrium of the foot and otherwise provides information about rotational instability as a function of the uncompensated rotational torques of the system acting on the foot. From this measure we may define a postural stability performance criterion:

*Stability Performance 1:* Average distance in the ground plane between the **FRI** point and the ground projected center of mass **GCoM** normalized by the distance traveled  $s$ .

$$\mathbf{J}_{s1}[\mathbf{q}, \dot{\mathbf{q}}, \mathbf{u}] = \frac{1}{s} \int_0^{t_f} \|\mathbf{GCoM} - \mathbf{FRI}\|^2 dt \quad (3)$$

This value alone is not sufficient to verify or design a dynamically stable control strategy, yet it may be combined with additional dynamic measures of the system such as the angular momentum which can provide a stability assessment during gait optimization, simulation, and on-line control.

A challenge for systems with limited power supply is to combine energy conserving motion with the robust, stability properties discussed previously. It has been witnessed in humans that steady-state forward walking approximates a minimum energy motion according to a dynamical model for the human body [17]. An attempt to reproduce smooth, natural motion should also take these factors into account.

*Energy Performance 1:* In legged systems where a high torque is generated by a large current in the motor, the primary form of energy loss is called the Joule thermal loss [15]. One may minimize the integral of this value over the gait:

$$\mathbf{J}_{e1}[\mathbf{u}] = \frac{1}{s} \int_0^{t_f} \sum_{i=1}^N R_i \left( \frac{u_i}{G_i K_i} \right)^2 dt \quad (4)$$

where  $R_i$ ,  $G_i$ ,  $K_i$ , and  $u_i$  are the armature resistance, gear ratio, torque factor, and applied torque for link  $i$  respectively, while  $s$  is the step length or total distance of one stride.

*Energy Performance 2:* Another efficiency cost criterion is the specific resistance  $\epsilon$  as used in [7]. This measures the output power in relation to the mass moved and the velocity attained and is a dimensionless quantity. Its integral over the gait cycle is a normalized form of the kinetic energy

$$\mathbf{J}_{e2}[\dot{\mathbf{q}}, \mathbf{u}] = \int_0^{t_f} \frac{\sum_{i=1}^N |u_i \dot{q}_i|}{mgv}, \quad (5)$$

where  $mg$  is the weight of the system,  $\dot{q}_i$  is the joint  $i$  angle velocity and  $v$  is the average forward velocity.

### Optimization of stability and performance indices

Our approach uses sophisticated numerical optimization techniques, which can incorporate the numerous modeling constraints to generate optimal trajectories [18]. The optimiza-

tion approach is based on a discretization of the control problem in time using direct collocation and its subsequent formulation as a nonlinear programming problem then solved with a sparse sequential quadratic programming algorithm. The resulting trajectories are tracked by trajectory following controllers in joint space.

### ONLINE COMPENSATION

When precalculated optimal control trajectories are applied in practice there usually occur some deviations of stability criteria or constraints due to modeling errors, link flexibilities, gear loss, backlash, joint control errors, and external disturbance forces acting on the robot from the environment. These may result in a degraded walking performance.

In this section a novel method termed *Jacobi Compensation* is proposed, which modifies precalculated trajectories in selected task coordinate directions in order to reduce stability criteria deviation and thereby improve walking performance. Task coordinates can be selected Cartesian directions of e.g. the hip coordinate or other task-dependent criteria such as the projected CoM, the FRI, etc.

The goal of the method is to move a specific set of coordinates  $\mathbf{p}_c \in \mathbb{R}^{m_c}$  of points on the humanoid, e.g. the center of the hips or an ankle, in the direction  $\Delta \mathbf{p}_c$  in Cartesian space to reduce deviations. The joint angles  $\mathbf{q}_t$ , e.g. obtained from a precalculated trajectory, are modified by  $\Delta \mathbf{q} = \mathbf{h}(\Delta \mathbf{p}_c)$ , where  $\mathbf{h}(\cdot)$  transforms the Cartesian motion  $\Delta \mathbf{p}_c$  into a joint space motion  $\Delta \mathbf{q}$ . As shown in Fig. 3, this correction  $\Delta \mathbf{q}$  is linearly superimposed with the joint configuration  $\mathbf{q}_t$  resulting in a new posture  $\mathbf{q}_d = \mathbf{q}_t + \Delta \mathbf{q}$  of the robot.

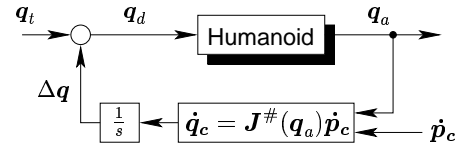


**Figure 3. Jacobi Compensation.** The precalculated trajectory is modified so that the motion of one part of the body is increased in direction  $\mathbf{p}_c$ .

The relationship between Cartesian motion and joint space motion is described by the Jacobian

$$\mathbf{J}(\mathbf{q}_a) = \begin{bmatrix} \frac{\partial \mathbf{p}_c}{\partial q_{a1}} & \dots & \frac{\partial \mathbf{p}_c}{\partial q_{aN}} \end{bmatrix} \in \mathbb{R}^{m_c \times N},$$

a function of the actual joint angles  $\mathbf{q}_a \in \mathbb{R}^N$  which maps the velocity  $\dot{\mathbf{q}}_c$  in joint space to the velocity  $\dot{\mathbf{p}}_c \in \mathbb{R}^{m_c}$  in Cartesian space according to

$$\dot{\mathbf{p}}_c = \mathbf{J}(\mathbf{q}_a) \dot{\mathbf{q}}_c. \quad (6)$$

To invert this relationship the pseudoinverse  $\mathbf{J}^\#(\mathbf{q}_a) := \mathbf{J}^T(\mathbf{J}\mathbf{J}^T)^{-1}$  minimizing the Euclidian norm  $\|\dot{\mathbf{q}}_c\|_2$  is used to obtain the joint motion; here,  $m_c < N$  is assumed for existence of a solution, i.e. the motion modification is along less task coordinates  $\mathbf{p}_c$  than degrees-of-freedom  $N$  of the

system. The velocity for correction of deviations is

$$\dot{\mathbf{q}}_c = \mathbf{J}^\#(\mathbf{q}_a) \dot{\mathbf{p}}_c, \quad (7)$$

which is integrated to obtain the position modification  $\Delta \mathbf{q}$  in joint space. Superimposing it with the precalculated trajectory  $\mathbf{q}_t$  allows one to adapt the trajectory to the actual requirements, cf. Fig. 3.

Depending on the control problem there exist a variety of possibilities to compute the correction velocity  $\dot{\mathbf{p}}_c$ . For the experiments described below, the velocity has been chosen proportional to the control error  $\dot{\mathbf{p}}_c = K \Delta \mathbf{p}_c$  of the task coordinates, where  $K$  is a positive definite (diagonal) matrix. Applications of this method are plentiful: In the experiments presented below the method has been used to alter the posture of the robot and thus modify precalculated trajectories to improve walking stability and performance. Other applications include the possibility to adapt precalculated gait trajectories to fit for walking on slopes.

## MECHANICAL DESIGN AND DYNAMICS

### Design considerations

One is faced with a difficult compromise in the design of an autonomous biped. Maximum agility and speed of locomotion require strong motors and gears. The actuators, though, must be as light as possible for autonomous operation and without extensive power consumption leading to heavy on-board batteries. A strategy for finding a good compromise between these conflicting goals using dynamic optimization has been presented with greater detail in [19]. The resulting architecture of the 80 cm humanoid robot is shown in Fig. 2.

The optimization criterion used was Energy Performance 1 of (4) subject to the complete biped dynamics for a rigid body model (1) and maximum input power constraints.

This investigation led to a 42V motor (20W) with a 66:1 gear ratio, see [19] for details.

### Hard- and software architecture

The mechanical biped construction (cf. Fig. 4) is based on linking elementary modules each consisting of motor, gear, pulse encoder, L-shaped base plate, and lever arm [19]. This prototype carries three batteries for the power supply of the motors, two of them visible on the picture at the height of the hips and below the waist joint. The third battery is located symmetrically behind the hips. The chosen Sony BP-L90A batteries provide a capacity of 90 Wh each, hence allowing for approximately 45 min autonomous walking.

For this prototype, a standard ATX mainboard with Athlon 1300 MHz CPU has been chosen providing enough computational power for motion control and additional tasks such as object recognition using a camera system. Its power is supplied by two Bebob Endura E-50S batteries.

The motors are accessed using an USB motion control board developed in the Control Systems Group in Berlin [19]. It consists of an 8 bit microcontroller including 3 USB endpoints, a 6 channel A/D converter and a 16 channel pulse-

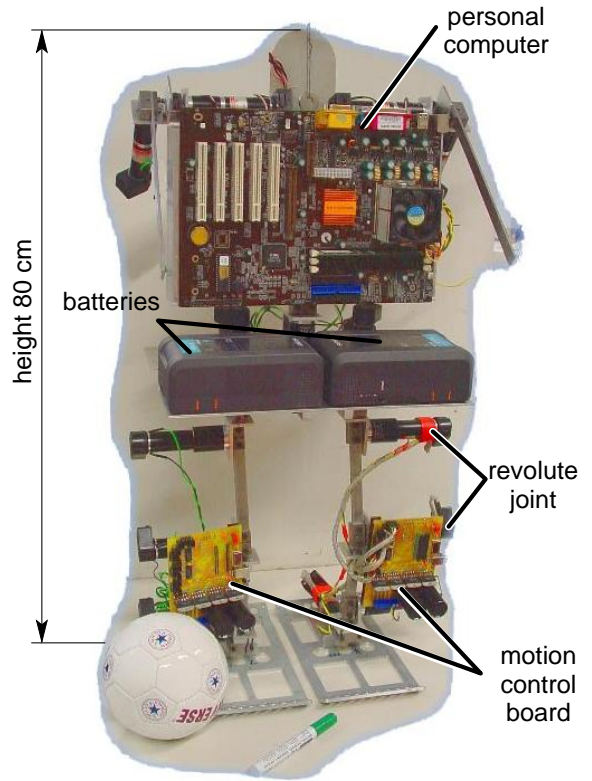


Figure 4. Mechanical Realization of the Biped Prototype

width modulator (PWM) admitting a motor load of up to 3 A at 55 V. The actual motor position is determined by evaluating the signals of pulse encoders attached to each motor. Up to 4 motors can be connected to each board weighing 170 g. In consideration of the USB control transfer mode, mean USB communication delay as well as microcontroller computational times required by USB service routines and PD control routines, PD control loops and communication runs have been designed and implemented at 250 Hz giving satisfactory control performance for this prototype.

A graphical user interface has been developed for rapid control prototyping. The control loop to be implemented is composed of ordinary SIMULINK blocksets, hence the migration from designing a controller in offline mode to evaluating it in an experiment is subject to substituting the system model by hardware in the loop which can also be accessed through SIMULINK blocksets.

## EXPERIMENTAL RESULTS

In the following, results of three experiments are described: In the first experiment, the trajectories generated by numerical optimal control, see above, are applied to the humanoid without modification as reference trajectories to local joint PD position controllers. The resulting walking performance is sometimes not stable due to modeling errors, gear backlash, and other effects. To improve the precalculated trajectories the Jacobi compensation method presented above is used to heuristically modify certain cartesian task coordinate points

of the robot in the second experiment. For the last experiment, the trajectories were modified manually by a teach-in of Jacobi compensation coordinates.

### Optimal Control Trajectory Experiments

The precalculated trajectories obtained by numerical optimization are applied to the humanoid as the reference trajectories to joint level PD position controllers. Fig. 5 shows the measured data of the left knee. Since the knee joint supports a significant part of the robot total weight, the load in the other joints are similar or less than the knee load.

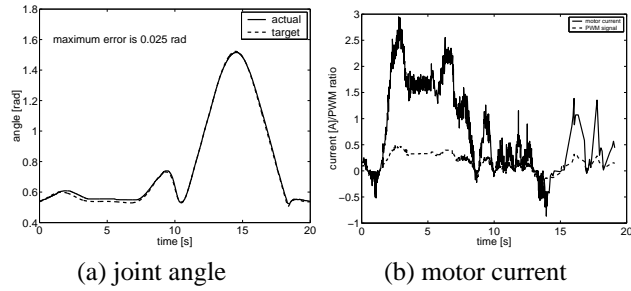


**Figure 5. First Experiments with Trajectory Following Control (knee joint of left leg).**

From Fig. 5(a) one can see, that the error of the commanded joint trajectory (dashed) and the measured position (solid) is quite small and does not exceed 0.025 rad for a complete stride. This validates the performance of the PD joint position control with a sampling rate of 250 Hz. The corresponding motor current (solid) and PWM ratio (dashed) are shown in Fig. 5(b). This plot similarly displays that the knee joint of the robot operates well below its limits with currents of 3 A (below the maximum H-bridge amplifier current of 4 A) and the PWM ratio always less than 50%. Another insight from this result is that the commanded PWM ratio is roughly proportional to the current in the motors, which indicates that in principle torque command control is realizable with the given hardware architecture.

Despite small errors in trajectory following in joint space, the robot gait was slightly tottering. Causes may be unmodeled backlash in the gears, link flexibilities, and other effects.

### Heuristic Compensation

In experiments with precalculated trajectories it turned out that the CoM is not shifted sufficiently far over the supporting leg. The observed effect is the tilting of the robot towards the swing leg as soon as the swing leg lifts off the ground. The application of the Jacobi Compensation method in this case increases robustness by a small modification of the hip position in lateral direction. This Jacobian is fed with a heuristically found compensation trajectory shown in Fig. 6 shifting the center of mass further over the supported area of the supporting leg. This heuristic compensation improved the walking behavior of the robot significantly.

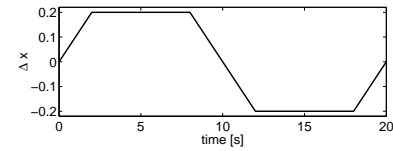


**Figure 6. Heuristic compensation of hip coordinate.**

### Teach-in Compensation

To further improve the Jacobi compensation reference, the desired  $\Delta \mathbf{p}_c$  has been trained in a teach-in cycle. The precalculated trajectory is stopped every 2 s and the operator modifies  $\Delta \mathbf{p}_c$  or directly at the joint level a  $\Delta \mathbf{q}$  to achieve a statically stable trajectory point by keyboard commands. These trained modifications of the precalculated trajectory are then linearly interpolated and superimposed with  $\mathbf{q}_i$  during normal operation. Again, the improvement of walking behavior, in particular stability, is significant as a result from this manual teach-in compensation method.

Fig. 7(a) again shows the desired and the measured trajectory of the left knee. As the robot now has to support its complete weight by the knee, the control error is higher than before; the maximum error is 0.042 rad. From Fig. 7(b) one can see, that the joint has reached its maximum load capabilities as the motor current saturates and the PWM ratio is close to 100%. This is not surprising, as the robot has been designed for fast locomotion where the required motor torque is smaller than the torque necessary for statically balancing on one leg.

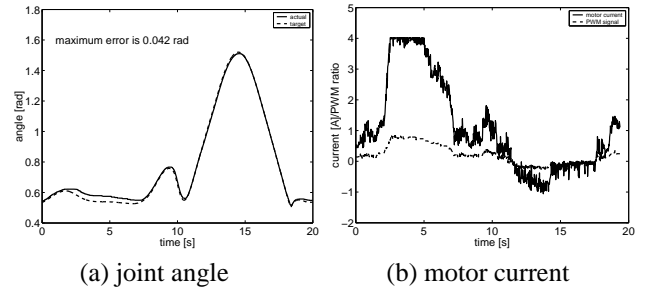


**Figure 7. Trajectory following with manually modified trajectories (knee joint of left leg).**

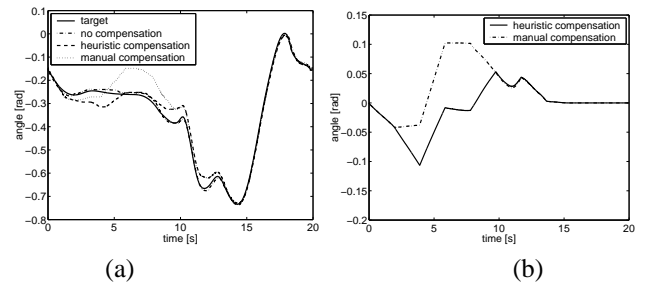


**Figure 8. Experimental result with teach-in compensation: (a) knee joint of left leg; (b) compensation trajectory  $\Delta \mathbf{q}_3$  for knee joint.**

The effect of the compensation is shown in Fig. 8(a) where the precalculated and modified trajectories of the left ankle joint are plotted. The compensation mainly affects the support phase, where the robot has to be balanced on the left leg.

## CONCLUSIONS

The development of autonomous bipedal robots requires results from many incompletely solved research areas including fast locomotion and agility. Modeling, simulation and optimization of complete dynamic models of the legged robot dynamics can greatly assist in making progress towards this goal on all levels of design, implementation and operation. We presented efficient approaches for modeling legged robot dynamics as well as measures for stability and performance of legged locomotion. Results for design considerations, trajectory optimization, and online compensation along selected task coordinates have been presented. Experimental results demonstrate the success of our approach to the control of the humanoid prototype.

Further steps will include the use of full multibody (inverse) dynamical models, motor and gear dynamics, and the development of ground contact sensors.

**Acknowledgments:** The authors gratefully acknowledge the support by the technical staff at Technical University of Berlin, in particular by Astrid Bergmann, Reinhold Kocur, Uwe Weidauer. Many thanks to all the students involved in the development of the prototype biped: Karsten Gänger, Stefan Schostan, Michael Bechdorf and Thorsten Hinzmann. A donation of 1000 EUR by the company Farnell is appreciated.

## REFERENCES

- [1] T. Arakawa and T. Fukuda, "Natural Motion Generation of Biped Locomotion Robot using Hierarchical Trajectory Generation Method Consisting of GA, EP Layers," in *Proceedings of the IEEE International Conference on Robotics and Automation*, (Albuquerque, New Mexico), pp. 211–216, 1997.
- [2] Ascher, U.M.; Petzold, L.R.: *Computer Methods for Ordinary Differential Equations and Differential-Algebraic Equations*. SIAM (1998)
- [3] C. Chevallereau, A. Formal'sky, and B. Perrin, "Control of a Walking Robot with Feet Following a Reference Trajectory Derived from Ballistic Motion," in *Proceedings of the IEEE International Conference on Robotics and Automation*, (Albuquerque, New Mexico), pp. 1094–1099, 1997.
- [4] Featherstone, R.; Orin, D.: *Robot Dynamics: Equations and Algorithms*. IEEE International Conference on Robotics and Automation (2000) 826–34
- [5] Y. Fujimoto and A. Kawamura, "Simulation of an Autonomous Biped Walking Robot Including Environmental Force Interaction," *IEEE Robotics and Automation Magazine*, vol. 5(2), pp. 33–42, June 1998.
- [6] Goswami, A.: Postural Stability of Biped Robots and the Foot-Rotation Indicator (FRI) Point. *International Journal of Robotics Research* **18**(6) (1999) 523–533
- [7] Gregorio, P.; Ahmadi, M.; Buehler, M.: Design, Control, and Energetics of an Electrically Actuated Legged Robot. *IEEE Transactions on Systems, Man and Cybernetics, Part B* **27**(4) (1997) 626–634
- [8] Hardt, M.; Helton, J.W.; Kreutz-Delgado, K.: Optimal Biped Walking with a Complete Dynamical Model. *IEEE Conference on Decision and Control* (1999) 2999–3004
- [9] Hardt, M.; von Stryk, O.: The role of motion dynamics in the design, control and stability of bipedal and quadrupedal robots. In: *Proc. RoboCup 2002 International Symposium*, June 24–25, 2002, Fukuoka, Japan (Springer-Verlag).
- [10] Helm, A.; Höppler, R.; Hardt, M.; von Stryk, O.: Development of a toolbox for model-based real-time simulation and analysis of legged robots. In: *Proc. GAMM Conference*, Augsburg, March 2002.
- [11] K. Hirai, "Current and Future Perspective of Honda Humanoid Robot," in *Proceedings of the IEEE/RSJ International Conference on Intelligent Robots and Systems IROS*, (Grenoble, France), pp. 500–508, 1997.
- [12] K. Hirai, M. Hirose, Y. Haikawa, and T. Takenaka, "The Development of Honda Humanoid Robot," in *Proceedings of the IEEE International Conference on Robotics and Automation*, (Leuven, Belgium), pp. 1321–1326, 1998.
- [13] M. Hirose, Y. Haikawa, T. Takenaka, and K. Hirai, "Development of Humanoid Robot ASIMO," in *IEEE/RSJ International Conference on Intelligent Robots and Systems (IROS) – Workshop 2*, (Maui, Hawaii), 2001.
- [14] Huang, Q.; Yokoi, K.; Kajita, S.; Kaneko, K.; Arai, H.; Koyachi, N.; Tanie, K.: Planning Walking Patterns for a Biped Robot. *IEEE Transactions on Robotics and Automation* **116** (1994) 30–36
- [15] Kimura, H.; Shimoyama, I.; Miura, H.: Dynamics in the Dynamic Walk of a Quadruped Robot. *Advanced Robotics* **4**(3) (1990) 283–301
- [16] Rodriguez, G.; Kreutz-Delgado, K.; Jain, A.: A Spatial Operator Algebra for Manipulator Modeling and Control. *International Journal of Robotics Research* **40** (1991) 21–50
- [17] Rose, J.; Gamble, J.G.: *Human Walking*, Baltimore, Williams & Wilkins (1994)
- [18] O. von Stryk "User's Guide for DIRCOL Version 2.1", Simulation and Systems Optimization Group, Technische Universität Darmstadt, [www.sim.informatik.tu-darmstadt.de/sw/dircol/](http://www.sim.informatik.tu-darmstadt.de/sw/dircol/).
- [19] D. Wollherr, M. Hardt, M. Buss, O. von Stryk, "Actuator selection and hardware realization of a small and fast-moving autonomous humanoid robot", in *Proc. 2002 IEEE/RSJ Int. Conf. on Intelligent Robots and Systems (IROS)* (Lausanne, Switzerland) 2002.